

Research Article

Mechanism and Procedure of Repeated Borehole Drilling Using Wall Protection and a Soft Structure to Prevent Rockburst: A Case Study

Yongliang He ^{1,2}, Mingshi Gao ^{1,2}, Xu Dong^{1,2} and Xin Yu ^{1,2}

¹School of Mines, China University of Mining and Technology, Xuzhou, Jiangsu 221116, China

²State Key Laboratory of Coal Resource and Safe Mining, China University of Mining and Technology, Xuzhou, Jiangsu 221116, China

Correspondence should be addressed to Mingshi Gao; cumt_gms@cumt.edu.cn

Received 3 November 2020; Revised 19 February 2021; Accepted 10 March 2021; Published 26 March 2021

Academic Editor: Hongwei Yang

Copyright © 2021 Yongliang He et al. This is an open access article distributed under the Creative Commons Attribution License, which permits unrestricted use, distribution, and reproduction in any medium, provided the original work is properly cited.

With the increasing mining depth of coal mines, the occurrence of rockburst, especially in mine roadways, is becoming critical as a severe dynamic disaster. This paper explores the stability control of deep mine roadways and solves the contradiction between the support and pressure relief of roadways by studying the use of an internal steel pipe for wall protection and a soft structure for energy absorption during repeated borehole drilling. Numerical simulations are performed to examine the effects of active support technology on the support structure during repeated drilling. Internal steel pipes can effectively prevent the support structure from being damaged. When the soft structure cracks, the energy transmitted from the rockburst to the roadway is significantly reduced. According to the deformation and failure characteristics of the surrounding rock of the 21170 roadway, the combination of anchor active support, hydraulic lifting shed support, and soft structure energy absorption is proposed. An engineering case study shows that the support method can effectively maintain the stability of the surrounding rock and ensure the safe mining of the working face. The proposed control method can provide reference for the prevention and control of rockburst in mine roadways under similar geological conditions.

1. Introduction

A rockburst represents a severe dynamic disaster that affects the safety and efficient production in underground projects such as coal mines [1, 2]. With the increase in the depths of coal mines, the rockburst severity has considerably increased, especially in China [3]. As of June 2019, 121 coal mines in production in China were identified as rockburst prone mines [4].

The mechanism of rockburst in coal mines is highly complex because of the complexity of the mechanical properties of coal and rock and diversity of geological conditions. Many theories on rockburst mechanisms have been proposed, including the strength theory [5], energy theory [6–8], bursting liability theory [9, 10], and rigidity theory [11, 12]. In recent years, considerable research on the

mechanism of rockburst has been conducted in China, and notable results have been achieved through the rockburst research and engineering practice. Zhang [13] proposed the theory of rockburst instability. Qi et al. [14] proposed the “three-factor” mechanism of rockburst, based on the results of friction and sliding instability tests on coal and rock. Dou et al. [15] proposed the strength weakening theory for rockburst. Pan [16] established the theory of rockburst initiation. Moreover, Pan [17] proposed the instability theory for the rockburst-induced disturbance response in coal mines. Rockburst prevention and control can be achieved by regulating the stress state or decreasing the generation of high stresses in the coal/rock mass structure. To this end, the main measures include reasonable mining of the protective layer, water injection in coal seams [18], pressure relief through large-diameter coal seam drilling and

coal seam blasting, roof softening through deep hole blasting and hydraulic fracturing, and the use of directional hydraulic fracturing. These measures can considerably reduce the risk of rockburst and effectively prevent the occurrence of rockburst disasters. According to preliminary statistics, 90.8% of rockburst accidents occurred in coal mine roadways [19]. However, only a few studies have focused on the support of roadways to prevent/control rockburst. From the perspective of rigid or flexible supports, support concepts for mine roadways have been established. The combinations of support technology currently used in coal mines include anchor net + anchor cable + steel arch support technology, steel U-bolt support technology, anchor + metal net + shotcrete + steel U-bolt support technology, energy absorption support technology, coupled rigid and flexible support technology [20], and “three-level support” technology [21]. In the anchor net + anchor cable + steel arch support technology, steel U-bolt support technology, and anchor + metal net + shotcrete + steel U-bolt support technology, only the support of the roadway is strengthened, and the pressure relief of the high stress roadway is not considered. The reinforcement of the roadway support increases the support cost and process and does not considerably influence the support effect of the roadway with rock burst. The energy absorption support technology, coupled rigid and flexible support technology, and “three-level support” technology involve filling a layer of energy absorbing material and adding energy absorbing materials with a weak stiffness between the surrounding rock and support, which can absorb a considerable amount of the impact energy and reduce the damage of the impact load on the support structure. However, this type of support can passively absorb only a small amount of energy, and if a large energy rockburst is encountered, the roadway may be critically damaged. The new support method proposed in this paper solves the contradiction between strong active support, pressure relief, and antiscour in rockburst roadway and can enhance the support and pressure relief effect of the rockburst roadway. Moreover, this approach can effectively maintain the strength and integrity of the surrounding rock of the roadway, thereby protecting it from damage; increase the stability of the surrounding rock of roadway wall, as the soft structure may crack again after high stress compaction; and protect the inner strong small structure from secondary damage of the borehole.

Rockburst occurrence changes the stress state in the coal and rock masses and may alter the generation of high stresses by transferring and releasing stress. In this study, focused on providing roadway support through energy absorption by soft structures, relevant technical measures are adopted to realize the stress transfer and stress release from coal and rock masses in mine roadways and effectively prevent the occurrence of rockburst. The anchor (cable)- + hydraulic lifting support + soft structure energy absorption technology is adopted. The technology of repeated borehole drilling and soft structure cracking is researched, and the contradiction between the support and pressure relief of a roadway under impact loading is coordinated, thereby enhancing the roadway performance.

2. Engineering Background of the Changcun Coal Mine

2.1. Geological Conditions. The Yima coal field, which is located in Yima, China (Mianchi County, Henan Province), is a thick coal field from the Mesozoic era. This region contains the Changcun, Yuejin, Qianqiu, Gengcun, and Yangcun coal mines. The coal seam in the Yima coal field is the middle Jurassic Yima formation, which contains 5 coal seams, among which the No. 2⁻¹ and 2⁻³ coal seams are generally minable. The mining depth of each coal seam is generally greater than 600 m, and the maximum depth is 1060 m. The lithologies of the coal seam roof and floor mainly include mudstone, sandstone, and conglomerate. The direct roof is generally mudstone, above which lies a sand conglomerate/argillaceous interbedded sandstone (average thickness = 166 m) layer, followed by an extremely thick gravel layer of the upper Jurassic period. Mining results in brittle fractures of the overlying hard plate, which easily cause dynamic disturbances in the roof. The F16 fault is a regional compressional and torsional thrust fault with a strike of approximately 110° (nearly east-west in orientation), an extension of approximately 45 km, a dip angle of 15–35° in the deep part and 75° in the shallow part, and a fault throw of approximately 50–500 m. The F16 fault connects with the Qianqiu mine in the north and extends into the Yangcun and Gengcun mines to the west and Changcun and Yuejin mines to the east, as shown in Figure 1.

2.2. Roadway Support. In the Yima mining area, the No. 2⁻³ coal seam is mainly mined. The mining roadway is generally arranged in the coal seam, 0.5 m of coal is reserved in the floor, and the section of the mine roadway is generally arched. A three-level support mode including an anchor net cable, 36 steel U-bolts, and a single hydraulic prop is generally adopted during the excavation of the mine roadway. The single hydraulic support is replaced by a hydraulic lifting frame or roadway supports during mining. A schematic and photograph of the three-level support system are shown in Figure 2.

2.3. Changcun Coal Mine. The surface of the Changcun coal mine is mostly covered with Quaternary loess. The ground elevation is 415–580 m, and the F16 reverse fault is a regional reverse fault that developed in the southeast region of the mine field. The direct roof of the coal seam is mudstone with a thickness of 16–45 m. The roof is mainly composed of conglomerate, fine sandstone, and mudstone, which can be permeated by water. The bottom of the coal seam is carbonaceous mudstone with a thickness of 0.5–6.0 m and a coal seam with a hardness of 1.5–2.0. The geological formations in the coal seam are presented in Figure 3.

During service, the 21170 working face is affected by the mining-induced dynamic pressure of the adjacent face. The west side consists of the three descending coal pillars of the 21 mining area, and the east side is the coal pillar of the F16 fault. The upper part of the working face is the 21150

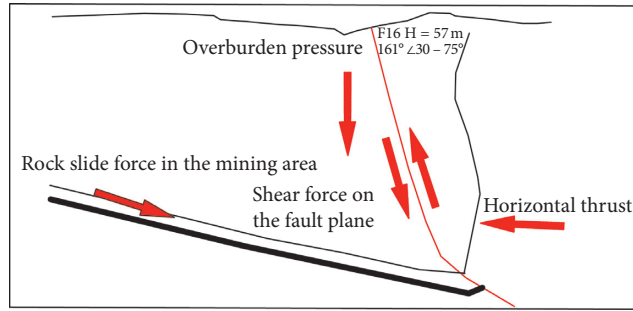
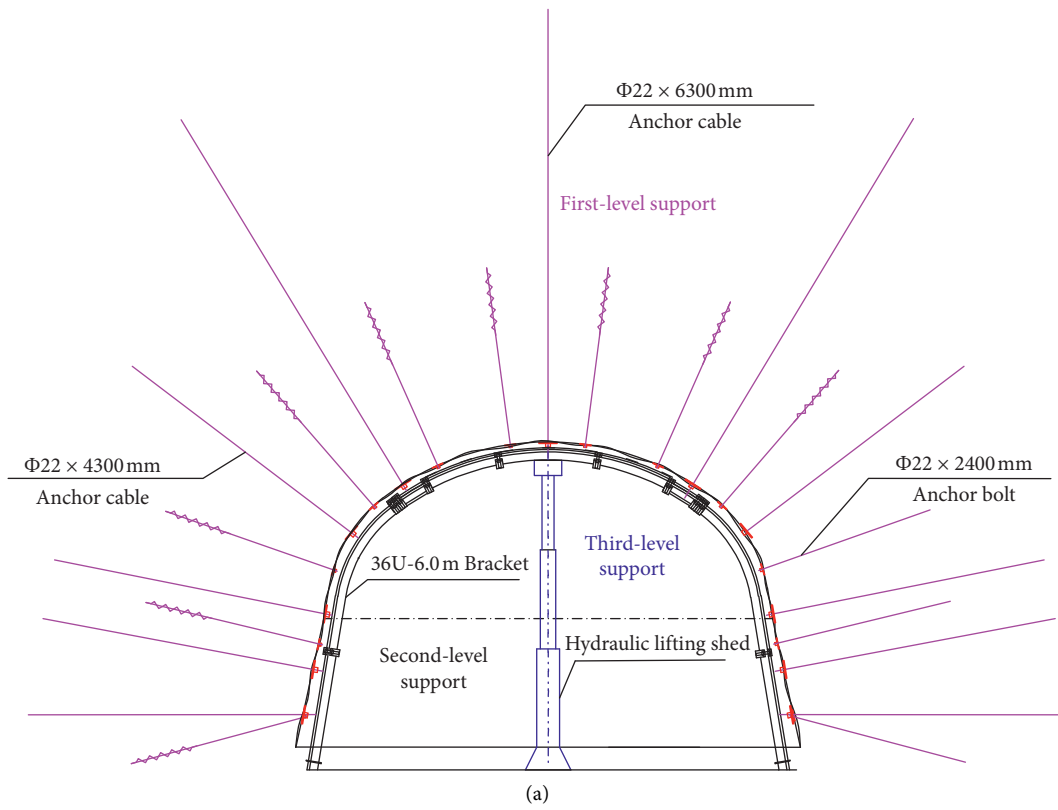


FIGURE 1: F16 fault diagram.



(b)

FIGURE 2: Three-level support of the surrounding rock. (a) Schematic. (b) Photograph.

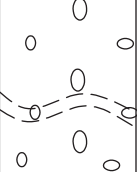
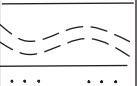

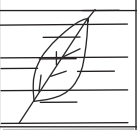

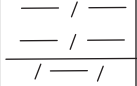

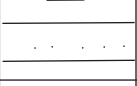

Drill hole	Depth (m)	Thickness (m)	Geological formation	Lithology name	Lithological characteristics
Roof	700.1	430		Conglomerate	Purplish red quartzite, quartz sandstone, gray green brown red igneous rock, with different diameters and sizes, argillaceous sand basement cemented, mixed with layered brown red siltstone
	720.6	23.5		Fine sandstone	Light gray spinning rock strip, wavy cross bedding, containing more nodular pyrite nodules, distributed along the layer, with dolomite broken in the section
	763.7	40.1		Mudstone	Plant fossils, partially carbonized, coarse-grained, dense and uniform below, with more siderite bands, horizontal bedding, and schistose pyrite at the bottom
	768.5	4.8		Mudstone	Muscovite sheet, containing siltstone locally, containing plant fragments and lamellibranchial fossils
Coal	779.7	12.0		Coal	Fibrous structure, light weight, mixed with carbonaceous mudstone and gangue
Floor	782.8	3.1		Mudstone	Black. High carbon content
	807.8	30.0		Argillite	Sandy claystone, containing angular quartzite small gravel and siderite, containing more plant root fossils. Slightly larger proportion
				Fine sandstone	Sandy claystone
812.9	5.1		Conglomerate	Quartz sandstone, shaly component, basal cementation	

FIGURE 3: Geological formations.

working face that has been stopped, and the lower part is the 21190 working face that has not been designed. The rock surrounding the roadway is mainly mudstone, which is easily weathered and broken, resulting in the rapid deformation of the roadway. The surrounding rock develops rapidly in the early stage of excavation. In addition to long-term creep, the overall deformation is large, and the roadway needs to be repaired after excavation. The deformation of the roadway mainly consists of two sides moving and floor heave. The 21170 working face is shown in Figure 4.

3. Borehole Wall Protection

Cracking of the soft structure is mainly caused by repeated drilling, blasting, water pressure [22], and air pressure [23, 24]. The complete rock mass is split into a loose state by an artificial method. The strength of the surrounding rock and support structure considerably influences the support of the roadway. Pressure relief or soft structure cracking

technology, such as drilling and blasting, transfers the stress from the roadway and weakens the strength of the roadway surrounding rock. After cracking, the structural integrity of the support structure is diminished, which deteriorates the stability of the roadway support. To protect the support structure from damage, the support structure is protected by an internal steel pipe. The control effect of the support structure and the internal steel pipe used for borehole protection on the strength of the surrounding rock and integrity of the support structure is analysed through numerical simulations; moreover, the stress and plastic zone of the surrounding coal and rock mass are investigated.

According to the geological conditions of the 21170 roadways, after the support of the roadway is completed, large-diameter pressure relief holes are drilled in the roadway. The drilling is performed perpendicular to the two sides of the roadway. The diameter of the hole is 110 mm, and the length and distance are 10 m and 1 m, respectively. The simulated roadway and support parameters are

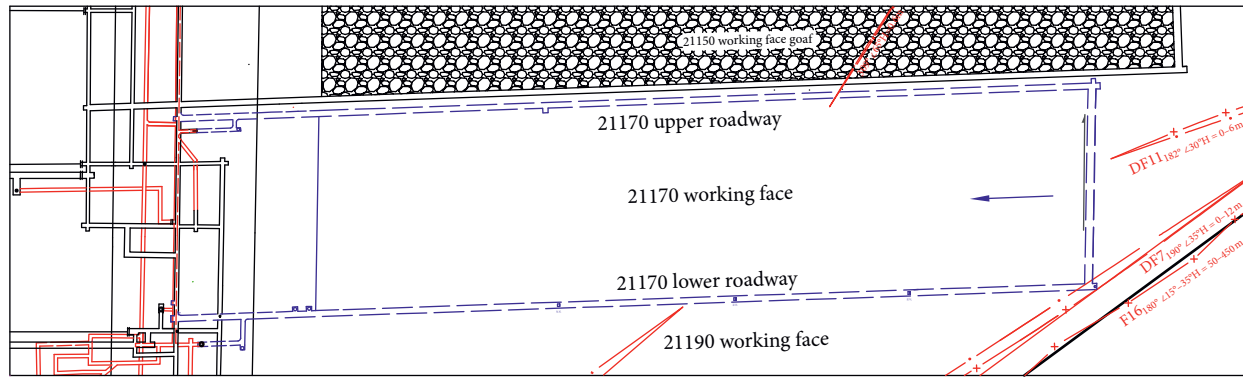


FIGURE 4: 21170 working face.

consistent with those on site. The steel pipe adopts a linear elastic constitutive model, with an elastic modulus of 210 GPa and wall thickness of 0.05 m. The steel pipe is modelled with cylindrical shell elements, for which the grid is as uniform as possible, and the grid in which the steel pipe and coal body are in contact is consistent. A contact surface is provided between the steel pipe and coal, and a hollow cylindrical grid is implemented at the contact surface on the steel pipe side. Figure 5 shows the simulation of the pressure relief hole.

Figures 6–11 show the stress and displacement states under the Mohr–Coulomb criterion. Almost no displacement is observed around the steel pipe; however, the displacement in the area around the steel pipe is 20 times larger when no steel pipes are used. The results of the stress calculation show that the stress in the coal cannot be released in the case of drilling with steel pipes installed, and the value is similar to the stress before drilling; in contrast, the stress in the coal is released when no steel pipes are used. Figure 12 shows the creep relations of the roadway during drilling with and without steel pipes. The plastic zone is larger when the borehole does not have a steel pipe. Under the action of high stress and large creep, the fracture range of the plastic zone further increases, thereby affecting the stability of the roadway support structure.

After the calculation balance of the roadway excavation, the plastic failure area of the surrounding rock is redefined into a new group by fish language. The Burger creep model is used as the constitutive model. The maximum time step is 0.04, the calculation time is 200, and the corresponding site age is 200 d. The creep variation and creep rate of the roadway are recorded in the whole process. Figure 13 shows the relationship curve of the creep variable, creep rate, and time.

4. Using a Soft Structure to Prevent Rockburst

4.1. Energy Absorption of a Soft Structure. A rockburst is a shock wave produced by either fracturing hard, thick strata during the mining process, or the movement and fracture of strata during the blasting process. The stress wave is directly transmitted to the roadway or working surface, and it may exceed the ultimate bearing capacity of the surrounding rock. Cracks in the surrounding rock induce instability and

failure of the support structure. Therefore, a soft structure with an energy-absorption function can be set outside the support area. The shock wave is considerably weakened through the scattering and absorption provided by the soft structure, and, consequently, the stability of the support structure can be maintained. Figure 14 shows the soft structure used for the mine roadway [25, 26]. The soft structure is essentially a wave absorption zone [27, 28]. The loose coal or rock formed by fracturing is used to absorb the energy generated by the rockburst.

In the process of transmission, an impact-induced stress wave may destroy the coal and rock mass. The energy generated when the impact occurs is denoted as E , the energy consumed in the transmission of the outer strong structure is denoted as E_1 , and the energy absorbed by the middle soft structure is denoted as E_2 . Therefore, the remaining energy that reaches the support structure is $E_3 = E - E_1 - E_2$. The energy absorption provided by the soft structure mainly includes the energy absorbed by the loose blocks and spatial scattering and that through rotation and rock reflection [29, 30], as shown in Figure 12. Energy is absorbed by the loose blocks because the dynamic shock wave requires more time to propagate through a fractured coal/rock mass than through a dense coal/rock mass, which decreases the shock wave velocity and vibration wave velocity; thus, the impact energy is reduced. Rotational energy absorption refers to the rotation/movement of the fractured coal/rock induced by the transmission of the dynamic waves, which transforms a portion of the impact energy to kinetic energy. Spatial scattering energy absorption refers to the energy absorbed through the formation of a broken area including fractured coal and rock. As the dynamic wave propagates, it is scattered to the surrounding broken area and expands continuously through the loose particles, thereby decreasing the energy of the dynamic wave. Rock-reflected energy absorption refers to the reflection and transmission phenomena of the dynamic wave in the broken area. After reflection, the energy of the transmitted dynamic wave is reduced, and the wave is dispersed. Therefore, the impact energy of the dynamic wave propagating to the roadway is reduced.

4.2. Numerical Simulation Development. A numerical simulation in FLAC3D is performed to examine the energy absorption and stress distribution of the soft structure in the

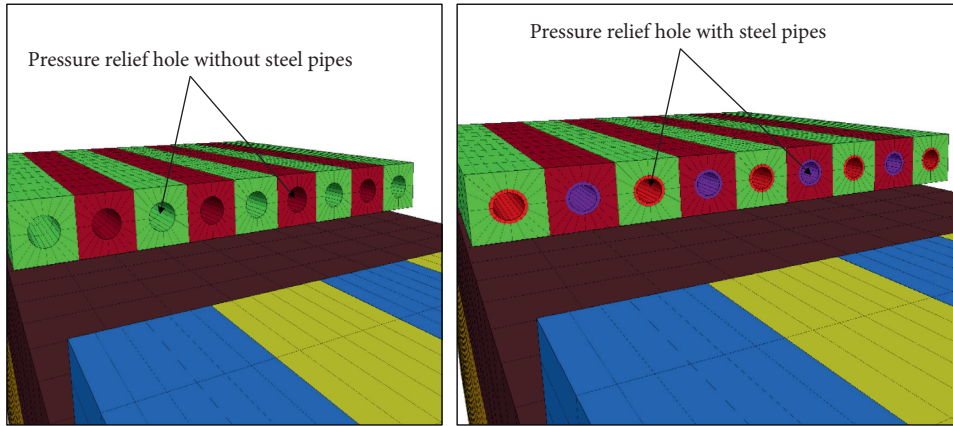


FIGURE 5: Pressure relief hole simulation.

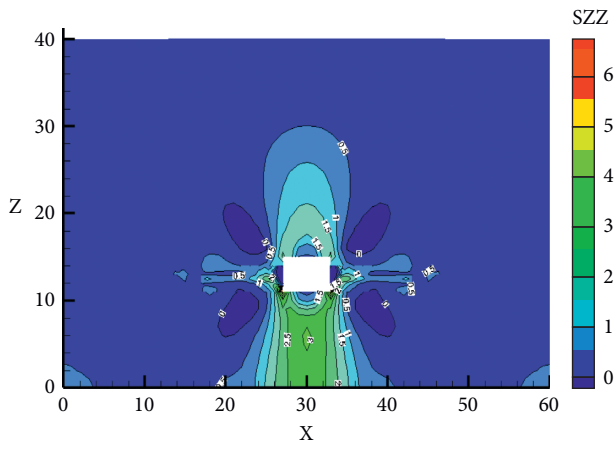


FIGURE 6: ZZ direction stress without steel pipes.

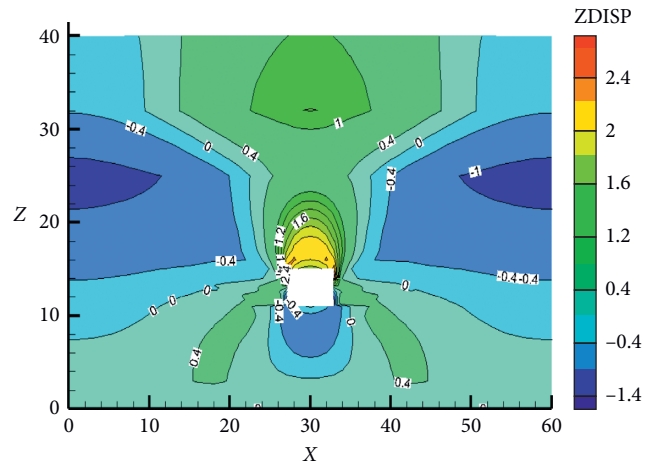


FIGURE 8: Z-displacement without steel pipes.

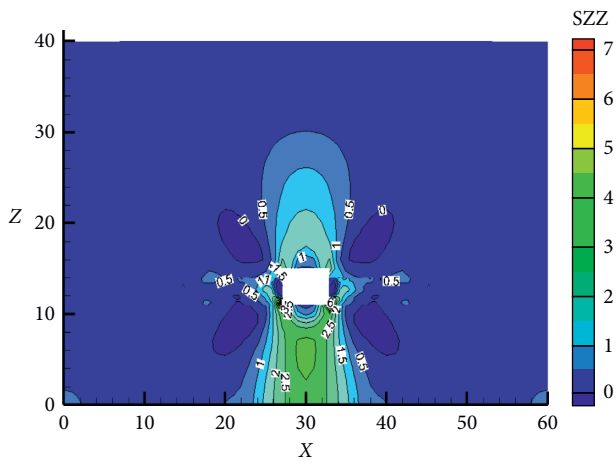


FIGURE 7: ZZ direction stress with steel pipes.

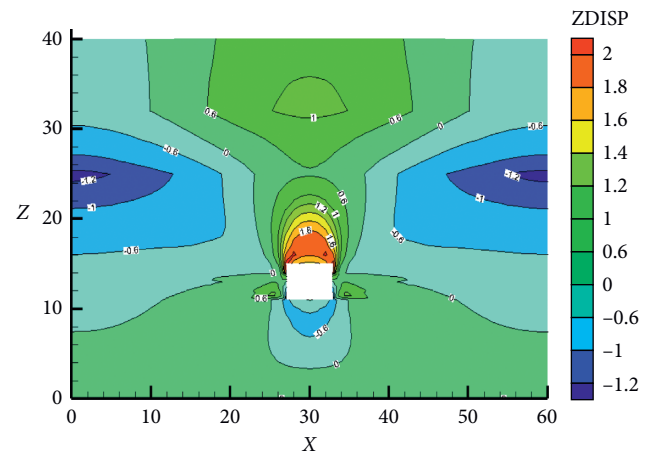


FIGURE 9: Z-displacement with steel pipes.

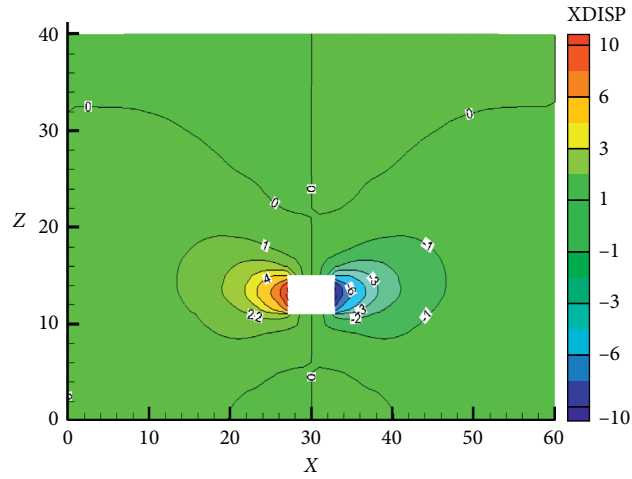


FIGURE 10: X-displacement without steel pipes.

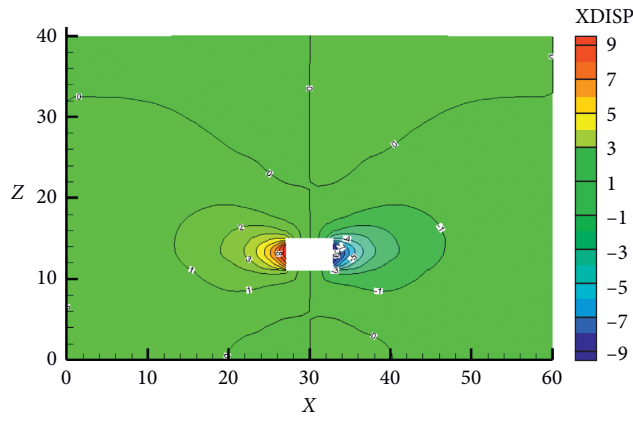


FIGURE 11: X-displacement with steel pipes.

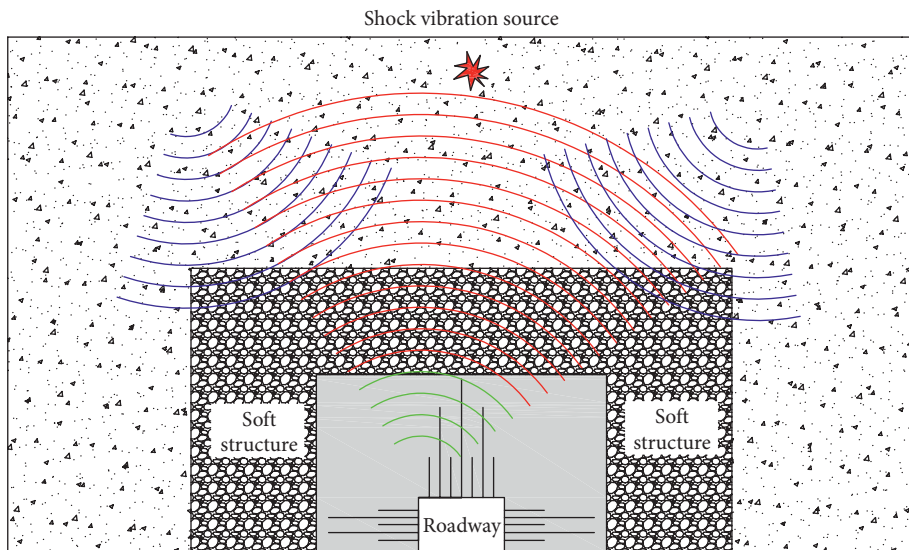


FIGURE 12: Soft structure used for a mine roadway.

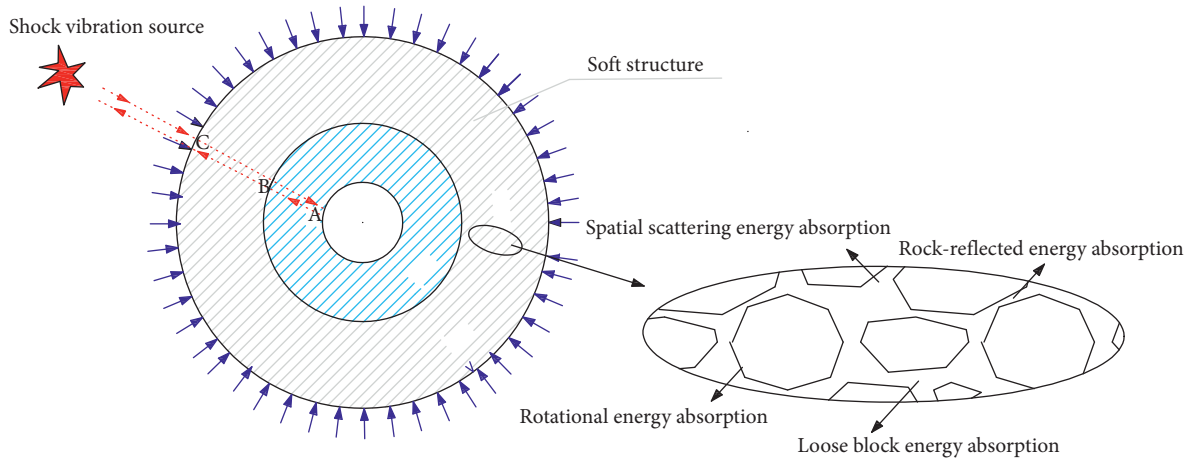


FIGURE 13: Roadway creep relations

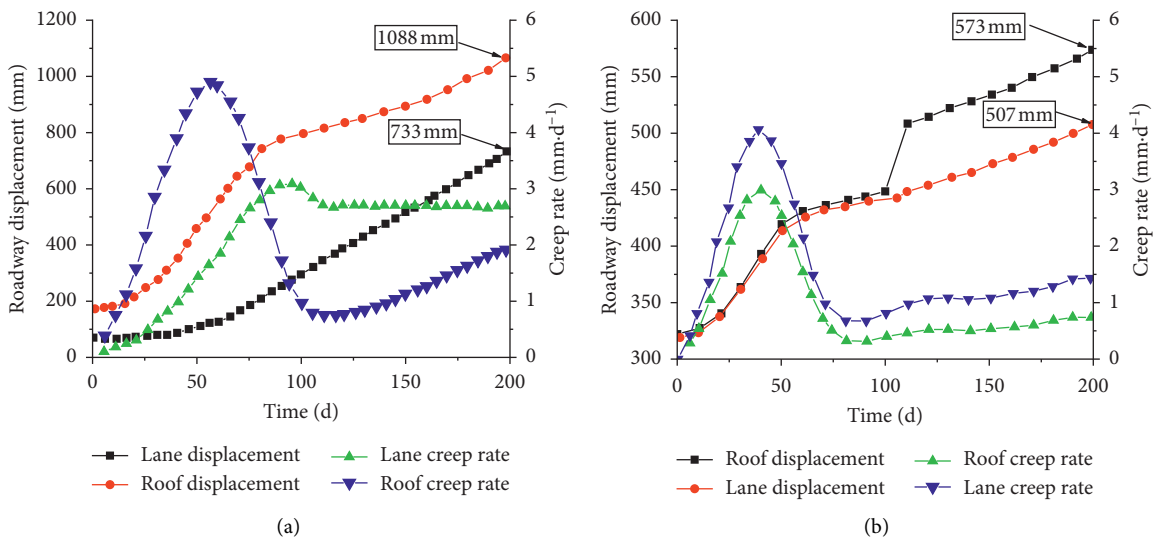


FIGURE 14: Roadway creep relations. (a) Roadway creep without steel pipes. (b) Roadway creep with steel pipes.

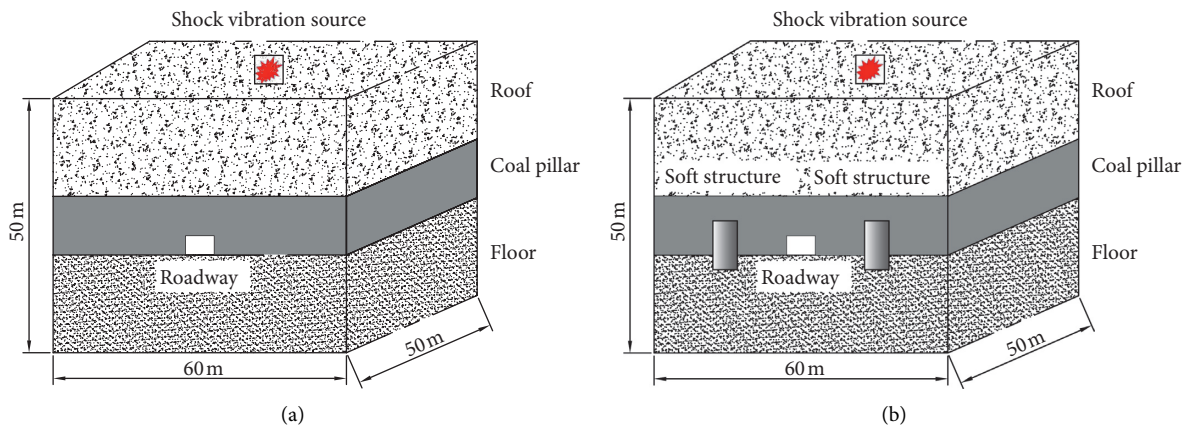


FIGURE 15: Numerical model. (a) Roadway without a soft structure. (b) Roadway with a soft structure.

roadway. According to the geological characteristics of the 21170 roadway, the numerical calculation model is as shown in Figure 15. This model has dimensions of $60\text{ m} \times 50\text{ m} \times 60\text{ m}$ ($X \times Y \times Z$), and a roadway with dimensions of $5.8\text{ m} \times 3.5\text{ m}$ is excavated in the centre of the model. According to the analysis of the soft structure with different widths and thicknesses, the soft structure is located 10 m outside the roadway support layer, with dimensions of $5\text{ m} \times 5\text{ m}$. The dynamic impact load is applied on the upper part of the model. The soft structure parameters can be set as 1% to 1/1000 of the rock parameters; we use 1% [31].

At the top of the model, a vertical stress of 17.5 MPa is applied to simulate the overburden. The horizontal and bottom sides are roller-constrained. The Mohr–Coulomb criterion is used to simulate the rock strata. Poisson's ratio of the coal and rock and the modulus of elasticity, cohesion, and tensile strength can be assumed to be 1.2–1.4 times and 0.1–0.25 times greater than those obtained through laboratory testing, respectively [32]. The average uniaxial compressive strength and average stiffness are 0.284 times and 0.469 times the values obtained in the laboratory [33]. According to the parameters determined experimentally, the distribution and mechanical parameters of the model are as shown in Table 1. The simulation involves the following steps. (1) Establish the model, set the boundary conditions, and balance the initial stress. (2) Excavate the roadway for static analysis. (3) Apply a dynamic load to simulate the effect of the roadway support without a soft structure. (4) Simulate the effect of the roadway support with a soft structure.

4.3. Impact Loading. The impact loading from a roof collapse on the roadway and time-history curve of the impact are shown in Figure 16. A roof collapse produces a dynamic load with an extremely short duration and high loading speed. The stress from this dynamic load has only a single peak, as it undergoes one loading and unloading action and later decays rapidly; no second stress wave occurs. The overall change trend is in the form of a pulse load. The maximum stress from the impact-induced dynamic load is 13.9 MPa, and the dynamic load duration is approximately 25 ms, of which the loading and unloading durations are 5 ms and 20 ms, respectively. The roof collapse rapidly produces a dynamic load greater than the static weight of the rock mass.

To describe the propagation of the stress wave in the model, the maximum grid width of the model is set as 1 m, which is less than 1/10 of the wavelength corresponding to the highest frequency of the wave. The boundary conditions are set as static boundaries, the mechanical resistance is Rayleigh damping, the minimum critical damping ratio is 0.005, and the minimum centre frequency is determined by the self-vibration frequency calculated using the model without damping under the action of gravity. The minimum centre frequency is calculated to be 8.0 Hz. The dynamic calculation time is 80 ms.

4.4. Numerical Simulation Effect. Before applying the dynamic load, the roadway strata are in a state of compressive stress, as shown in Figure 17. Because the dynamic loading wave is

reflected and refracted at the interface of the roadway strata during propagation, the reflected stress wave and unloading effect of the impact load are superposed, which transforms the vertical stress in the roadway from a compressive stress to a tensile stress. The low tensile strength of rock and action of the dynamic load can easily lead to tensile failure of the rock floor. After the soft structure cracks, the vertical stress is reduced, and the soft structure attenuates the stress wave and protects the roadway from damage. Figures 18 and 19 show the simulation results of the roadway displacement. The roadway displacement is large under the action of the dynamic load in the roadway without a soft structure. However, after the soft structure cracks, the soft structure absorbs the dynamic loading wave, and the roadway support structure is not damaged. Figure 20 shows the plastic zone under the impact load, in which the tensile and shear failures occurred in the roadway. Primarily existing shear and tension failure units can be observed around the roadway support without the soft structure; in contrast, existing and new shear failure units can be observed around the roadway with the soft structure.

The rockburst caused by the large-scale collapse of the rock mass on the roadway and the dynamic loading and stope pressure are superposed in the form of a vector. The result of this stress superposition causes oscillations in the roadway stress field. Since the stress state during dynamic loading shifts from compression to tension, when the tensile stress is greater than the tensile strength of the rock in the floor layer, cracks occur along the tensile surface. Under the superposition of the dynamic load and mining support pressure, the shear stress is concentrated, and the rock stratum is damaged by compression and shear. The impact of a large-scale rock mass promotes the development of fractures in the roadway strata, which causes a significant increase in the range and depth of damage in the roadway strata. The cracks created in the soft structure facilitate wave absorption and energy dissipation, as the formation and propagation of these cracks help absorb a portion of the energy from the dynamic wave.

5. Engineering Case Study

5.1. Roadway Support. As shown in Figure 21, $\Phi 22 \times 2500$ mm anchors are used for the roof, for which the individual spacing is 900 mm, and the row spacing is 800 mm; $\Phi 18.9 \times 5300$ mm anchor cables are arranged along the roadway, with an individual spacing of 1.5 m and row spacing of 1.6 m; and $\Phi 18.9 \times 8000$ mm anchor cables are arranged along the roadway, with an individual spacing of 2.5 m and row spacing of 1.6 m. Two rows of horizontal anchor cable beams are constructed in the middle of the two sides and near the bottom. The anchor cable has dimensions of $\Phi 18.9 \times 5300$ mm, the steel beam is 3.2 m long, and the hole spacing is 1.6 m. After installing the anchor and mesh support, a hydraulic lifting shed is built along the centre of the roadway to strengthen the support.

5.2. Soft Structure Cracking. The repeated cutting method is used to weaken the two sides of the roadway to create the “soft structure” to absorb the dynamic and static energy. The

TABLE 1: Mechanical parameters of the coal and rock used in the numerical model.

Rock strata	Thickness (m)	Density (kg/m^3)	Bulk modulus (GPa)	Shear modulus (GPa)	Cohesion (MPa)	Friction angle ($^\circ$)
Conglomerate	5	2440	3.06	1.66	2.1	34
Fine sandstone	20	2540	4.5	2.8	2.5	23.25
Carbon mudstone	2	2600	4.2	0.47	3.5	32
Coal	12	1350	0.433	0.2	7.0	33
Fine sandstone	3	2570	1.01	0.70	2.6	26
Mudstone	40	2450	2.82	0.57	3.5	32

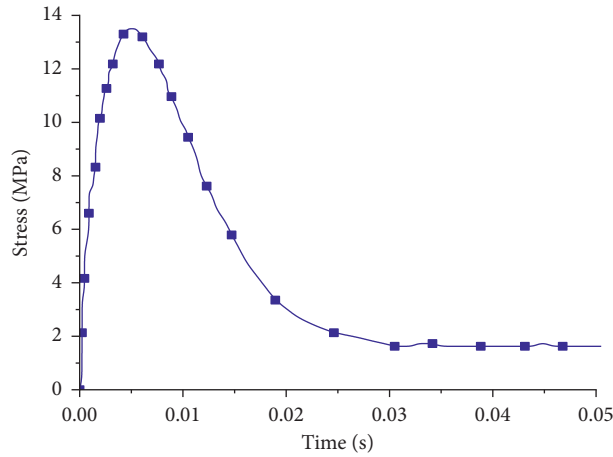


FIGURE 16: Time-history curve of the impact load.

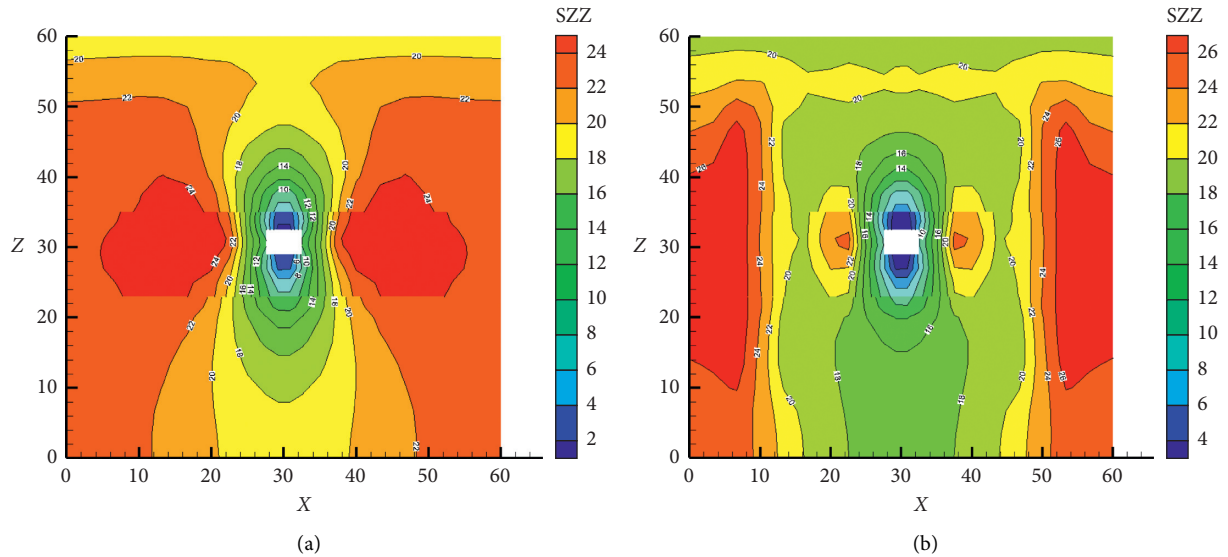


FIGURE 17: Stress field analysis. (a) Roadway without a soft structure. (b) Roadway with a soft structure.

drilling machine prepares several pressure-relief holes in the designated positions of the coal and rock on the left and right sides of the roadway. The diameter of the drilling hole is 110 mm, and the spacing between the openings of the pressure-relief holes is 3 m. A 10 m steel pipe is inserted in the borehole to protect the strong structure from damage, which helps strengthen the strong structure in the roadway. We continue drilling from the pressure relief borehole inside

the steel tube and crack the coal and rock in the roadway by using the drill pipe deep in the pressure relief borehole. After the cracking, the coal and rock are interconnected to form the soft anti-impact structure of the two sides of the roadway. After the two sides of the roadway are compacted under the action of the pressure of coal and rock mass, the coal and rock masses are cracked and relieved through repeated cycles of inserting steel tubes without destroying

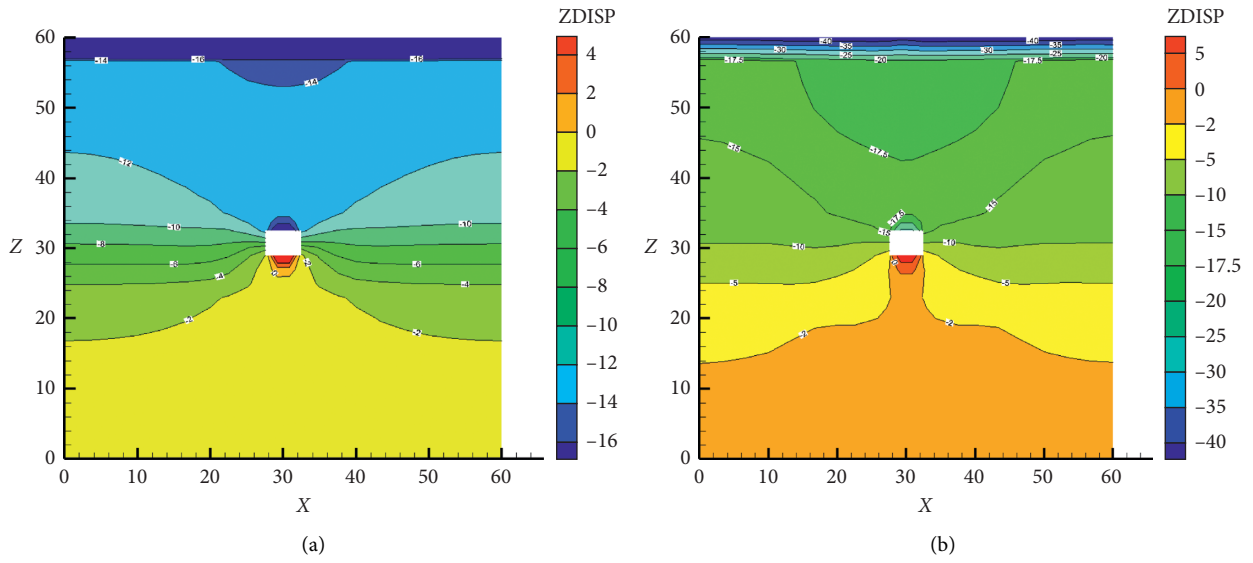


FIGURE 18: Z-displacement analysis. (a) Roadway without a soft structure. (b) Roadway with a soft structure.

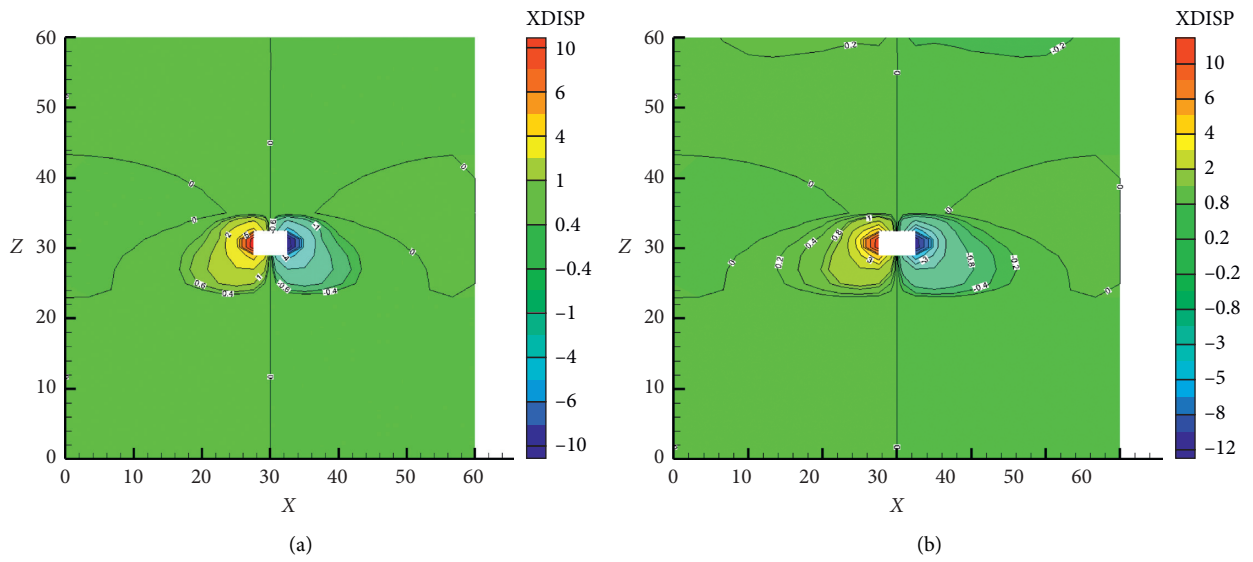


FIGURE 19: X-displacement analysis. (a) Roadway without a soft structure. (b) Roadway with a soft structure.

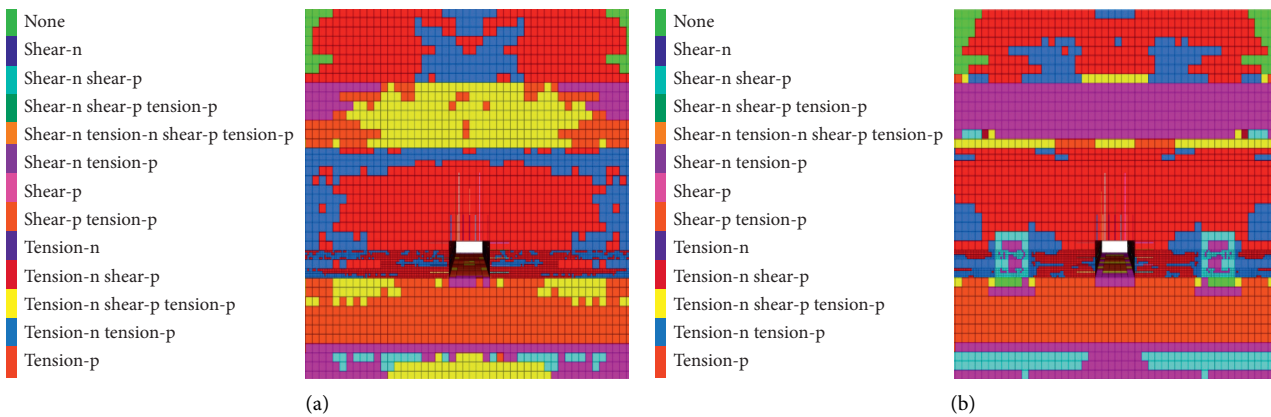


FIGURE 20: Plastic zone. (a) Roadway without a soft structure. (b) Roadway with a soft structure.

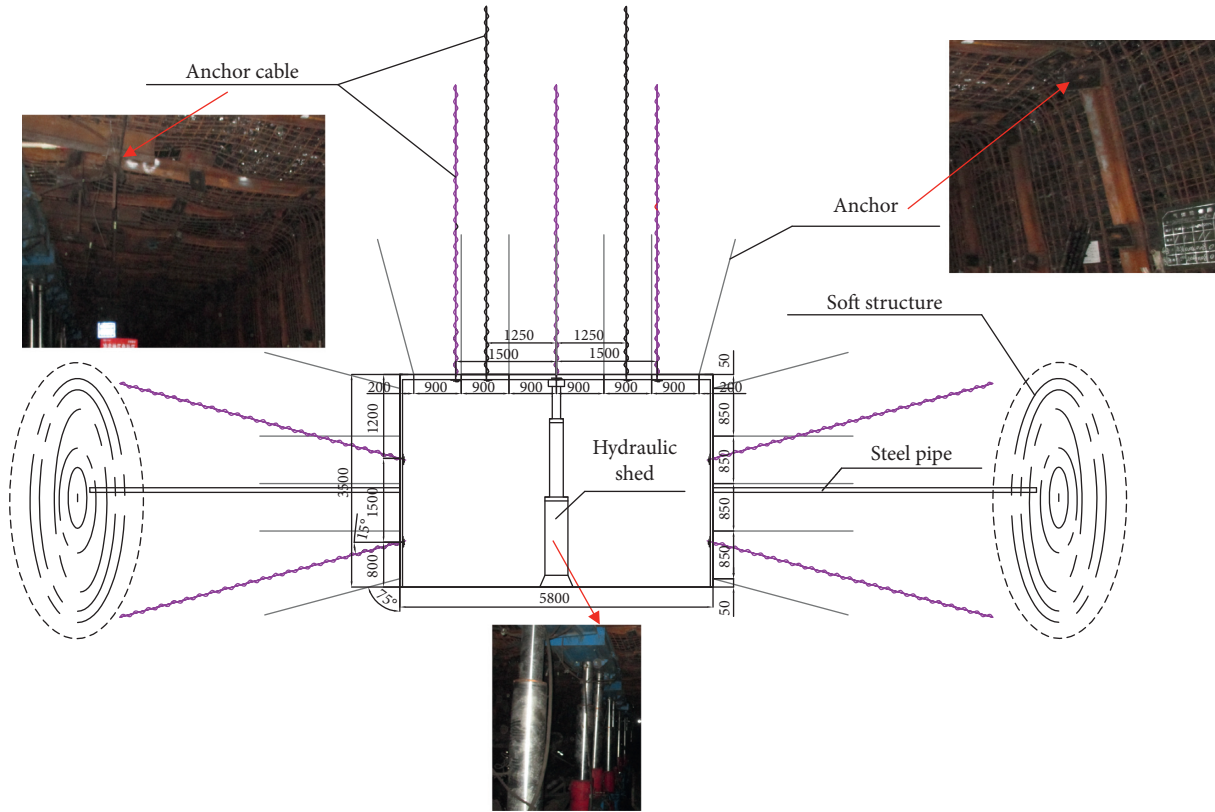


FIGURE 21: Roadway support parameters.

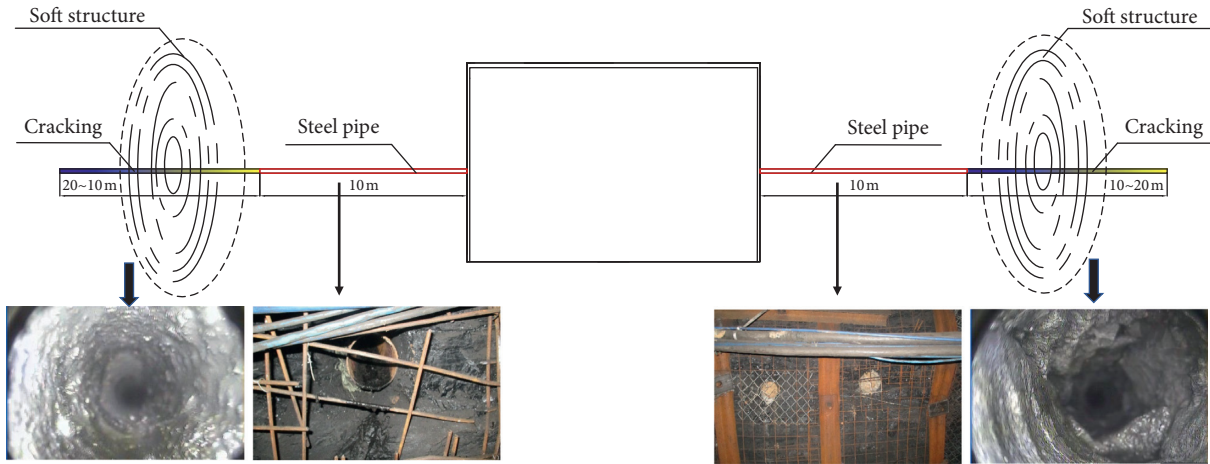


FIGURE 22: Soft structure construction.

the strong and small structures in the roadway. The support layer of the roadway does not enlarge the loose circle of the coal and rock mass under the action of pressure relief drilling.

According to the observation of the mine pressure, holes (depth and diameter of 20 m and 110 mm, respectively) are drilled on both sides of the roadway, and 10 m long steel pipes are placed in the holes. The steel pipe can be formed by the butt joint of a short steel pipe and screws. In the outer end of the steel pipe, the loose structure of coal is formed in the process of drilling. After the soft structures of the two

sides of the roadway are compacted under the pressure of the coal and rock mass, drilling is again performed through the steel pipe into the pressure relief borehole to crack the coal and rock mass of the roadway. According to the compaction of the soft structure of the two sides of the roadway, the coal and rock mass of the roadway is repeatedly cracked many times. In this process, the left and right sides of the roadway do not expand the loosening ring of the coal and rock mass under the action of pressure relief drilling, which protects the support structure while cracking the soft structure. The cracking of the soft structure is shown in Figure 22.

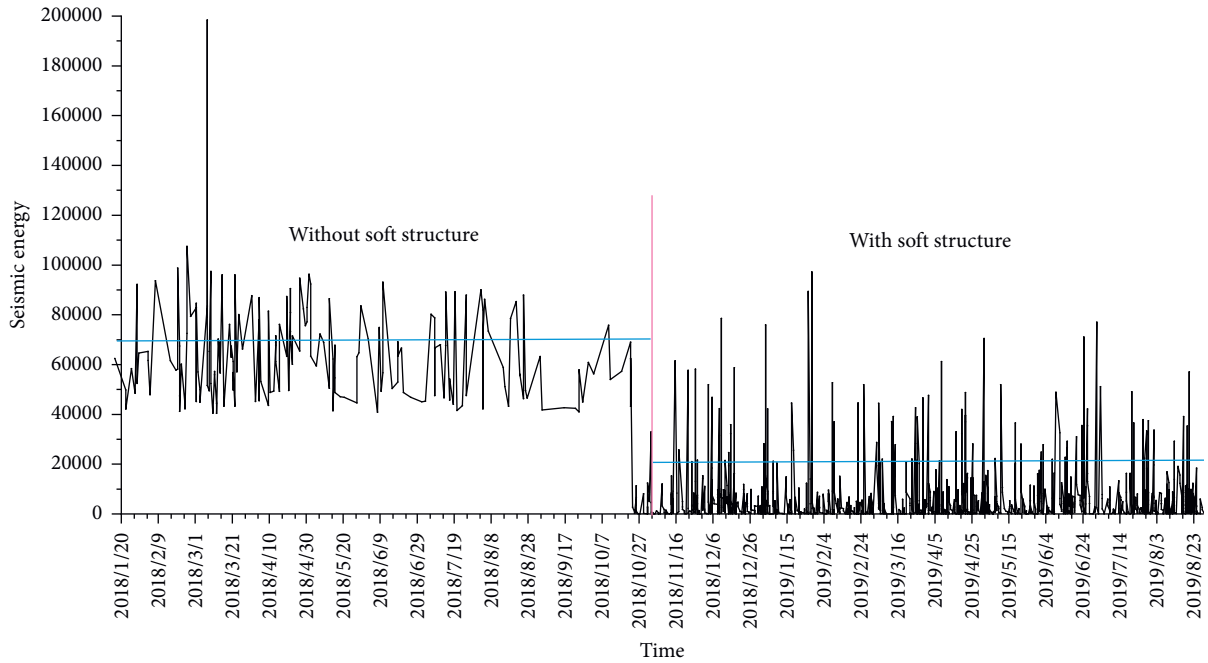


FIGURE 23: Microseismic energy monitoring before and after soft structure construction.

TABLE 2: Comparison of roadway supports.

	Previous	Present
Roof		
Roadway		
Overall		

Figure 23 shows the microseismic energy monitoring of the roadway before and after the soft structure cracking. It can be noted that the energy monitored is significantly reduced after the soft structure cracking. The stress in the coal body can be noted to be transferred or absorbed, which effectively reduces the roadway damage caused by the high stress and rockburst.

5.3. *Support Effect.* The active support of the stable anchorage bearing circle of the roadway support and pressure relief of the middle soft structure provide satisfactory stress support conditions for the roadway. The internal steel pipe used for borehole protection can repeatedly crack the middle soft structure while protecting the support structure from damage, which prevents not only the crack expansion of the

loosening circle of the support structure but also the overall instability of the support of the roadway, thereby solving the contradiction between the support and pressure relief of the roadway. Table 2 compares the roadway support effects. The support parameters significantly enhance the roadway support situation. The selection of the support parameters is reasonable, which effectively controls the roof separation and deformation of the rock surrounding the roadway.

6. Conclusions

The combination of internal steel pipe borehole protection, repeated borehole drilling, and soft structure cracking is studied. The soft structure can solve the contradiction between the support and pressure relief of roadways. Numerical simulations are performed to study the active support of the support structure and energy absorption of the soft structure. The internal steel pipe used for borehole protection effectively prevents the support structure from being damaged. When the soft structure cracks during drilling, the energy from a rockburst transmitted to the roadway is significantly reduced. The main conclusions are as follows:

- (1) The use of a soft structure for mine roadways is examined, the support structure mechanism of the surrounding rock is analysed, and the deformation of the rock surrounding the roadway is effectively controlled. The deformation and failure of the rock surrounding the roadway are closely related to the strength of the support structure.
- (2) The soft structure can transfer or absorb high stresses and high energy, thereby attenuating the shock wave. The energy absorption provided by the soft structures is analysed, which mainly includes loose block energy absorption, rotational energy absorption, spatial scattering energy absorption, and rock-reflected energy absorption.
- (3) The internal steel pipe used for borehole protection can protect the support structure from being weakened by pressure relief drilling. Under a high stress and large creep, the fracture range of the plastic zone in the roadway without a steel pipe increases to 1033 mm, according to the results of the numerical simulation. The soft structure facilitates wave absorption and energy dissipation and can mostly absorb the shock wave.
- (4) To control the stability of the surrounding rock in deep coal mines with high stresses, strong pressure relief and large creep under the condition of multifactor superposition, and failure mode coupling, the deformation and failure mechanism and failure characteristics of the surrounding rock in such roadways are studied. The combination of anchor active support + hydraulic lifting support + soft structure energy absorption is proposed. A steel pipe is embedded in the support structure to protect the structure from damage; this configuration can retain the integrity of the coal body in the roadway and ensure the support effect.

Data Availability

The data used to support the findings of this study are available from the corresponding author upon request.

Conflicts of Interest

The authors declare that they have no conflicts of interest regarding the publication of this study.

Acknowledgments

The authors would like to acknowledge the National Natural Science Foundation of China (Grant no. 51564044) and State Key Laboratory of Coal Resources and Safe Mining, China University of Mining and Technology (Grants nos. SKLCSRSM15X02 and SKLCSRSM18KF004).

References

- [1] W. D. Ortlepp and T. R. Stacey, "Rockburst mechanisms in tunnels and shafts," *Tunnelling and Underground Space Technology*, vol. 9, no. 1, pp. 59–65, 1994.
- [2] C. Wu, L. Dou, and M. Zhang, "A fuzzy comprehensive evaluation methodology for rock burst forecasting using microseismic monitoring," *Tunnelling and Underground Space Technology*, vol. 80, pp. 232–245, 2018.
- [3] Y. Jiang, Y. Zhao, and H. Wang, "A review of mechanism and prevention technologies of coal bumps in China," *Journal of Rock Mechanics and Geotechnical Engineering*, vol. 9, pp. 180–194, 2017.
- [4] Q. Qi, L. I. Yizhe, S. Zhao et al., "Seventy years development of coal mine rockburst in China: establishment and consideration of theory and technology system," *Coal Science and Technology (in Chinese)*, vol. 47, no. 9, pp. 1–40, 2019.
- [5] A. N. Romashov and S. S. Tsygankov, "Generalized model of rock bursts," *Journal of Mining Science*, vol. 28, no. 5, pp. 420–423, 1993.
- [6] N. G. W. Cook, "The failure of rock," *International Journal of Rock Mechanics and Mining Sciences & Geomechanics Abstracts*, vol. 2, pp. 389–403, 1965.
- [7] AV. Lovchikov, "Difference in rockburst hazard in ore and coal mines," *Iop Conference*, vol. 134, pp. 12–17, 2018.
- [8] Y. Xu and M. Cai, "Influence of strain energy released from a test machine on rock failure process," *Canadian Geotechnical Journal*, vol. 55, pp. 777–791, 2018.
- [9] A. Kidybiński, "Bursting liability indices of coal," *International Journal of Rock Mechanics and Mining Sciences*, vol. 18, no. 4, pp. 295–304, 1981.
- [10] J.-A. Wang and H. D. Park, "Comprehensive prediction of rockburst based on analysis of strain energy in rocks," *Tunnelling and Underground Space Technology*, vol. 16, no. 1, pp. 49–57, 2001.
- [11] T.-H. Ma, C.-A. Tang, S.-B. Tang et al., "Rockburst mechanism and prediction based on microseismic monitoring," *International Journal of Rock Mechanics and Mining Sciences*, vol. 110, pp. 177–188, 2018.
- [12] Z. H. Chen, C. A. Tang, and R. Q. Huang, "A double rock sample model for rockbursts," *International Journal of Rock*

- Mechanics and Mining Sciences*, vol. 34, no. 6, pp. 991–1000, 1997.
- [13] M. Zhang, “Instability theory and mathematical model for coal rock bursts,” *Chinese Journal of Rock Mechanics and Engineering*, vol. 6, no. 3, pp. 197–204, 1987.
- [14] Q. Qi, Y. Shi, and T. Liu, “Mechanism of instability caused by viscous sliding in rock burst,” *Journal of China Coal Society (in Chinese)*, vol. 21, no. 2, pp. 34–38, 1997.
- [15] L. Dou, C. Lu, Z. Mou et al., “Intensity weakening theory for rockburst and its application,” *Journal of China Coal Society (in Chinese)*, vol. 30, no. 6, pp. 690–694, 2005.
- [16] J. Pan, “Theory of rockburst start-up and its complete technology system,” *Journal of China Coal Society (in Chinese)*, vol. 44, no. 1, pp. 173–182, 2019.
- [17] Y. Pan, “Disturbance response instability theory of rockburst in coal mine,” *Journal of China Coal Society (in Chinese)*, vol. 43, no. 8, pp. 2091–2098, 2018.
- [18] Yi Xue, Z. Cao, and W. Shen, “Destabilization and energy characteristics of coal pillar in roadway driving along gob based on rockburst risk assessment,” *Royal Society Open Science*, vol. 6, pp. 1–20, 2019.
- [19] Y. Jiang and Y. Zhao, “State of the art: investigation on mechanism, forecast and control of coal bumps in China,” *Chinese Journal of Rock Mechanics and Engineering*, vol. 34, no. 11, pp. 2188–2204, 2015.
- [20] Y. Pan, X. Liu, and Z. Li, “The Model of energy-absorbing coupling support and its application in rock burst roadway,” *Journal of Mining and Safety Engineering*, vol. 28, no. 1, pp. 6–10, 2011.
- [21] Q. Qi, Y. Pan, L. Shu et al., “Theory and technical framework of prevention and control with different sources in multi-scales for coal and rock dynamic disasters in deep mining of coal mines,” *Journal of China Coal Society*, vol. 43, no. 7, pp. 1801–1810, 2018.
- [22] A. Pak and D. H. Chan, “Numerical modeling of hydraulic fracturing in oil sands,” *Scientia Iranica*, vol. 15, no. 5, pp. 516–535, 2008.
- [23] Z. Huang, S. Zhang, R. Yang et al., “A review of liquid nitrogen fracturing technology,” *Fuel*, vol. 266, pp. 1–15, 2020.
- [24] F. Bagheri, “Regulation of hydraulic fracturing of shale gas formations in the United States,” *Pepperdine Policy Review*, vol. 6, pp. 1–13, 2013.
- [25] M. Gao, L. Dou, and N. Zhang, “Strong-soft-strong mechanical model for controlling roadway surrounding rock subjected to rock burst and its application,” *Rock and Soil Mechanics*, vol. 29, no. 2, pp. 359–364, 2008.
- [26] Y. He, M. Gao, H. Zhao, and Y. Zhao, “Behaviour of foam concrete under impact loading based on SHPB experiments,” *Shock and Vibration*, vol. 2019, Article ID 2065845, 13 pages, 2019.
- [27] M. Gao, H. Zhao, Y. Zhao, X. Gao, and X. Wang, “Investigation on the vibration effect of shock wave in rock burst by in situ microseismic monitoring,” *Shock and Vibration*, vol. 2018, pp. 1–14, Article ID 8517806, 2018.
- [28] M. Gao, Y. Zhao, and X. Chen, “Destruction mechanism of rock burst in mine roadways and their prevention,” *Disaster Advances*, vol. 6, no. 5, pp. 34–43, 2013.
- [29] Y. Wu, F. Gao, J. Chen, and J. He, “Experimental study on the performance of rock bolts in coal burst-prone mines,” *Rock Mechanics and Rock Engineering*, vol. 52, no. 10, pp. 3959–3970, 2019.
- [30] L. Dai, Y. Pan, and A. Wang, “Study of the energy absorption performance of an axial splitting component for anchor bolts under static loading,” *Tunnelling and Underground Space Technology*, vol. 81, no. 81, pp. 176–186, 2018.
- [31] M.-S. Gao, *Strong-soft-strong Control Principle for Controlling Roadway Surrounding Rock Subjected to Rock burst*, China University of Mining and Technology Press, Xuzhou, China, 2011.
- [32] Z.-L. Li, X.-Q. He, L.-M. Dou, D.-Z. Song, and G.-F. Wang, “Numerical investigation of load shedding and rockburst reduction effects of top-coal caving mining in thick coal seams,” *International Journal of Rock Mechanics and Mining Sciences*, vol. 110, pp. 266–278, 2018.
- [33] N. Mohammad, D. J. Reddish, and L. R. Stace, “The relation between in situ and laboratory rock properties used in numerical modelling,” *International Journal of Rock Mechanics and Mining Sciences*, vol. 34, no. 2, pp. 289–297, 1997.